MADRID
inter.noise 2019
June 16 - 19
NOISE CONTROL FOR A BETTER ENVIRONMENT

Dynamic Analysis of Phononic Crystal Curved Beam Using the Spectral Transfer Matrix Method

Goto, Adriano M.[1]
Nobrega, Edilson. D[2]
Dos Santos, José Maria C.[3]

University of Campinas (UNICAMP)
Rua Mendeleyev, 200, C. Univ. "Zeferino Vaz", Campinas-SP, Brazil.

ABSTRACT

Phononic Crystals (PCs) are artificial materials created by a periodic repetition of a unit-cell, made with an arrangement of high impedance variation system (scatterers, shape, material property), in order to obtain band gaps. Elastic phonic crystals are structural systems tailored using the same concept as the PCs. Curved beams are important structural elements that can be found in many engineering applications, such as aerospace structures, bridges, tunnels and roof structures. The dynamic analysis of structures such as, arches, helical springs, rings, and tires can be modeled using curved beam theory. They can be modeled using Transfer Matrix (TM) method, which relates the left and right sides of the structure. In general, the transfer matrix can be obtained by partitioning the dynamic stiffness matrix. However, due to the inversion of some sub-matrix, this process may generate an ill-conditioned transfer matrix. One away to avoid this problem is using the Spectral Transfer Matrix (STM) method, where the transfer matrix can be obtained directly from the space-state model of the system. In this paper, a curved beam phononic crystal is modeled using a two material property unit-cell, organized periodically along the curve and evaluated by STM. PCs work as a "wave filter", which can attenuate mechanical vibrations at a certain frequency band called *bandgap*. Dispersion diagrams and forced responses are calculated for the curved beam phononic crystal. The wavenumbers and wave modes were obtained using the Floquet-Bloch theorem, and the forced response is calculated by the wave expansion.

Keywords: Curved Beam, Phononic Crystal, Bandgap, Spectral Transfer Matrix Method.

[1]gotoadriano8@gmail.com
[2]edilsonnobre@gmail.com
[3]zema@fem.unicamp.br

1. INTRODUCTION

The dynamical analysis of curved beams have been subject of several investigation due the considerable number of application in engineering, such as aerospace structure, bridges, tunnels and roofs. The curved beam theory also can be extended to modeling of tires [1]. The governing equations of curved beam can be formulated for different beam theories (Euler-Bernoulli, Timoshenko and Extended Timoshenko) and applied for analysis of free vibration and wave propagation [2, 3, 4, 5]. Phononic crystals (PCs) are artificial materials that exhibit periodic repetitions of a unit-cells. The changes in the unit-cell are high impedance variation system (scatterers, geometry, material property) in order to obtain frequency bands where the waves are prohibited to propagate. THis frequency bands are called as stop bands or bandgaps. This arrangement allows the structure to have the attribute of "wave filtering", where the mechanical vibration is attenuated in a certain frequency band of bandgap. The prediction of bandgap regions for a particular PC arrangement can be done with the dispersion diagram of the cell (wavenumber $\times$ frequency), which provides the wave behavior (propagating or non-propagating) inside the structure. Several analytical and numerical methods have been developed for calculating the band structure of PCs, such as the transfer matrix (TM) method [6], the plane wave expansion (PWE) method [7], the finite difference time domain (FDTD) method [8], the multiple scattering theory (MST) [9], the finite element (FE) method [10], the wave finite element (WFE) method [11, 12, 13] and the spectral element method (SE) method [14, 13]. In general, phononic crystal are modeled using Transfer Matrix (TM) method, which relates the left and right sides of the structure. The transfer matrix can be obtained by partitioning the dynamic stiffness matrix. However, due to the inversion of some sub-matrix, this process may generate an ill-conditioned transfer matrix. One away to avoid this problem is using the Spectral Transfer Matrix (STM) method, where the transfer matrix can be obtained directly from the space-state model of the system. In this paper, a curved beam phononic crystal is modeled using a two material property unit-cell, organized periodically along the curve and evaluated by STM.

2. MATHEMATICAL FORMULATION

2.1 Spectral Transfer Matrix Method

The STM is an alternative approach to derive the spectral element without need the exact wave solutions of the frequency-domain governing equations [15]. The method is based on the representation of the governing equations in a set of first order ordinary differential equations. By introducing a state vector $\mathbf{y}$, the system is transformed into a first-order ordinary differential equation given by:

$$\frac{d\mathbf{y}}{dx} = \mathbf{G}\,\mathbf{y}, \tag{1}$$

where $\mathbf{G}$ is a coefficient matrix, $\mathbf{y} = \{\mathbf{u} \quad \mathbf{F}\}^T$ is the state-vector, $\mathbf{u}$ is the displacements vector and $\mathbf{F}$ is the internal forces vector. The solution of the Equation 1 is:

$$\mathbf{y}(x) = e^{\mathbf{G}x}\,\mathbf{y}(0). \tag{2}$$

Applying for a 1-D structural member of length L it has:

$$\mathbf{y}(L) = e^{\mathbf{G}L}\,\mathbf{y}(0) = \mathbf{T}\,\mathbf{y}(0), \tag{3}$$

where $\mathbf{T} = e^{\mathbf{G}L}$ is the transfer matrix. It is a matrix exponential that can be solved using any method based on Cayley-Hamilton theorem [16].

2.2 Curved beam model

For a curved beam, the displacement and the internal forces can be rewritten in according to the radial and circumferential orientation. The curved beam model is a combination of elementary rod and Euler-Bernoulli beam theories. The straight beam longitudinal and transversal displacements becomes circumferential and radial in the curved beam, respectively, and the rotation remains the same. Figure 1 shows the in-plane displacements () and internal forces of a curved beam.

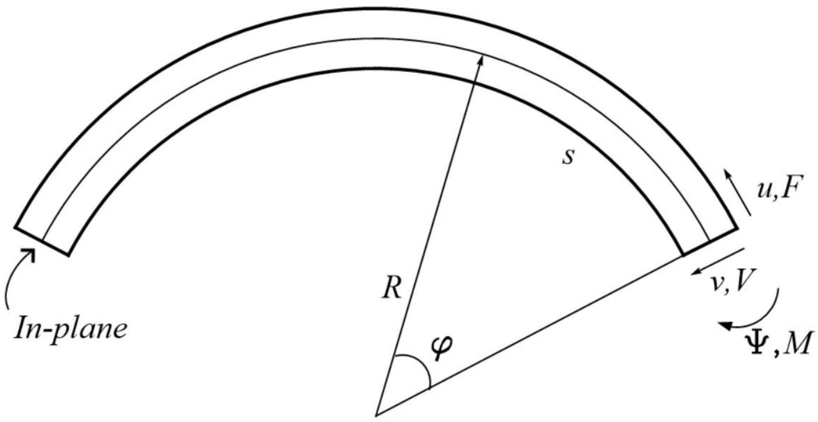

Figure 1: Displacements and internal forces in a curved beam.

The coupled governing equation in frequency domain of a curved beam is given by [14, 1]:

$$
\begin{aligned}
&\left(EA + \frac{EI}{R^2}\right)\frac{du}{ds} + \rho A\omega^2\, u + \frac{1}{R}\left(-EA\frac{dv}{ds} + EI\frac{d^3v}{ds^3}\right) = 0, \\
&EI\frac{d^4v}{ds^4} + \frac{EA}{R^2}v - \rho A\omega^2\, v + \frac{1}{R}\left(-EA\frac{du}{ds} + EI\frac{d^3u}{ds^3}\right) = 0,
\end{aligned}
\tag{4}
$$

where u, v and are the cir is circumferential displacemente E,A, ρ, ω and I are, respectively, the Young's modulus, cross-section area, mass density, circular frequency and the moment of inertia. R indicates the curved beam radius.

The Equation 4 can be rewritten as:

$$
\begin{aligned}
&\frac{d}{ds}\left[EA\left(\frac{du}{ds} - \frac{v}{R}\right)\right] + \frac{EI}{R}\left(\frac{d^3v}{ds^3} + \frac{1}{R}\frac{d^2u}{ds^2}\right) + \rho A\omega^2\, u = 0 \\
&\frac{d}{ds}\left[-EI\left(\frac{d^3v}{ds^3} + \frac{1}{R}\frac{d^2u}{ds^2}\right)\right] + \frac{EA}{R}\left(\frac{du}{ds} - \frac{v}{R}\right) + \rho A\omega^2\, v = 0
\end{aligned}
\tag{5}
$$

The internal forces and rotation are:

$$F = EA\left(\frac{du}{ds} - \frac{v}{R}\right) \qquad V = -EI\left(\frac{d^3v}{ds^3} + \frac{1}{R}\frac{d^2u}{ds^2}\right),$$
$$M = EI\left(\frac{d^2v}{ds^2} + \frac{1}{R}\frac{du}{ds}\right) \qquad \psi = \frac{dv}{ds}. \tag{6}$$

The Equation 5 can be rewritten using the terms of internal forces, Equation 6, as:

$$\begin{aligned}
\frac{du}{ds} &= \frac{v}{R} + \frac{F}{EA} & \frac{dF}{ds} &= -\rho A\,\omega^2\,u + \frac{V}{R}\\
\frac{dv}{ds} &= \psi & \frac{dV}{ds} &= -\rho A\,\omega^2\,v - \frac{F}{R}\\
\frac{d\psi}{ds} &= -\frac{v}{R^2} - \frac{F}{R\,EA} + \frac{M}{EI} & \frac{dM}{ds} &= -V
\end{aligned}$$
$$\Downarrow \tag{7}$$
$$\frac{d}{dx}\begin{Bmatrix} u\\ v\\ \psi\\ F\\ V\\ M\end{Bmatrix} = \underbrace{\begin{bmatrix} 0 & \frac{1}{R} & 0 & \frac{1}{EA} & 0 & 0\\ 0 & 0 & 1 & 0 & 0 & 0\\ 0 & -\frac{1}{R^2} & 0 & -\frac{1}{R\,EA} & 0 & \frac{1}{EI}\\ -\rho A\,\omega^2 & 0 & 0 & 0 & \frac{1}{R} & 0\\ 0 & -\rho A\,\omega^2 & 0 & -\frac{1}{R} & 0 & 0\\ 0 & 0 & 0 & 0 & -1 & 0\end{bmatrix}}_{\mathbf{G}} \begin{Bmatrix} u\\ v\\ \psi\\ F\\ V\\ M\end{Bmatrix}.$$

The transfer matrix is computed from Equation 3. This expression is showed in the Appendix.

3. MODELING OF ONE-DIMENSIONAL PHONONIC CRYSTALS

The phononic crystal (PC) unit cell contains two materials, which are polymer and steel. Figure 2 shows a schematic view of the phononic crystal and the unit-cell composed by a sequence of polymer, steel and polymer.

For a 1D phononic crystal, the Equation 3 can be partitioned in terms of left and right side of unit-cell as:

$$\mathbf{y}_r^{(m)} = \mathbf{T}_c\,\mathbf{y}_l^{(m)}, \tag{8}$$

with the subscripts r and l corresponding to the right and left nodes of the $m-th$ unit-cell. While $\mathbf{T}_c$ represents Its transfer matrix, calculated by:

$$\mathbf{T}_c = \mathbf{T}_1\,\mathbf{T}_2\,\mathbf{T}_1, \tag{9}$$

where the subscript 1 and 2 indicates the polymer and steel proprieties, respectively.

Using the coupling relation at the unit-cells interface ($\mathbf{y}_l^{(m+1)} = \mathbf{y}_r^{(m)}$) and applying Floquet-Bloch theorem [17] it has:

$$\mathbf{T}_c\,\mathbf{y}_l^{(m)} = e^{-i\cdot kL}\,\mathbf{y}_l^{(m)} \quad \text{or} \quad \mathbf{T}_c\,\mathbf{y}_l = e^{-i\cdot kL}\,\mathbf{y}_l. \tag{10}$$

The eigenproblem of Equation 9 is solved and the eigenvalues produces dispersion diagrams and the eigenvectors the wave modes. It is important to note that the

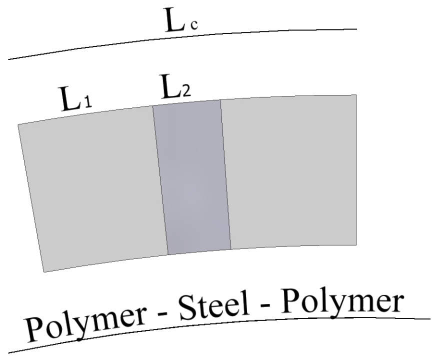

Figure 2: Curved beam: phononic crystal unit-cell composed by polymer-steel-polymer.

eigenvectors and eigenvalues are independent of the unit-cell position in the structure. To each n degree of freedom has $2n$ eigenvalues that can be ordered appropriately into two groups: $|e^{\mu_j}| \leq 1$, $j = 1, 2, \ldots, n$ indicate waves propagating to the right and $|e^{-\mu}| \geq 1$, $j = 1, 2, \ldots, n$ correspond to waves traveling to the left. Therefore, wave amplitudes can be obtained as follows [18]:

$$\mathbf{y}^{(m)} = \sum_{j}^{n} e^{-i \cdot k_j L} \Phi_j \, \mathbf{y}_j^{(m)} \qquad \text{with } m = 1, 2, 3 \ldots N_c, N_{c+1}, \tag{11}$$

where $j = 1, 2, \ldots, n$ with n as the number of eigenvalues and N_c the total number of unit-cells.

4. NUMERICAL RESULTS

4.1 Validation of the STM method

Initially, the STM method is compared with the Spectral Element (SE) method to validate the transfer matrix obtained for curved beam. It is considered a curved beam of rectangular cross-sectional area of width $b = 100$ mm and height $h = b/10$. The radius of curvature is $R = 10h$ and the hoop length $S = R\pi$. The boundary conditions is showed in the Figure 3. The structures was excited with unity force in the circumferential direction. The choice of the orientation force is arbitrary. The material properties corresponds to polymer with Young's modulus $E = 3$ GPa, density $\rho = 1340\,\mathrm{kg\,m^{-3}}$, Poisson's ration $\nu = 0.4$ and damping factor $\eta = 0.002$. Figure 4 shows the dispersion curve and the forced response at the excitation point for a curved beam calculated by STM and SE methods. The forced response is evaluated at the excitation point. As seen, the STM approach presents good agreement with the SE method. Particularly, the STM has an advantage for not require the exact wave solution of the governing equation.

4.2 Analysis for PC curved beam

A numerical example of a phononic crystal curved beam with two different material is showed. It is considered a curved beam of rectangular cross-sectional area of width $b = 20$

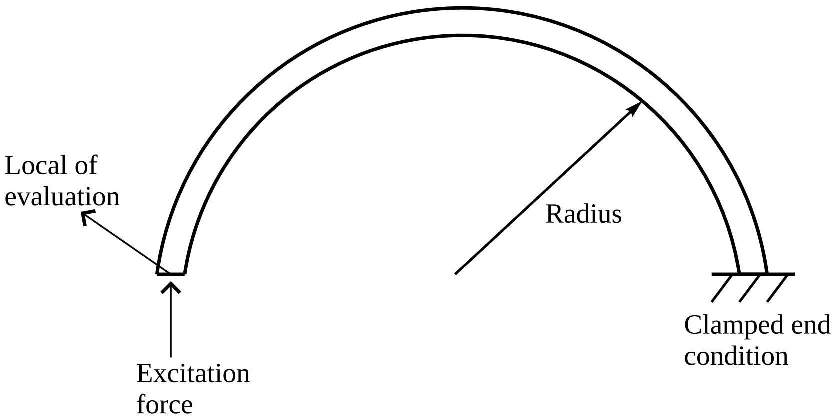

Figure 3: A cantilever curved uniform beam with excitation at circumferential orientation.

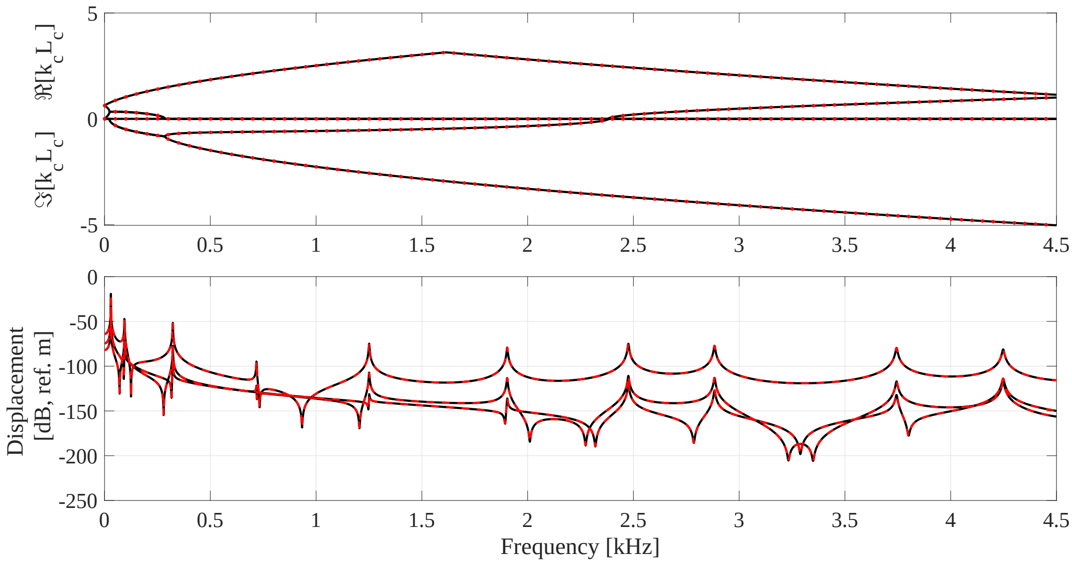

Figure 4: Comparison of the SE and STM method for a curved beam. STM (—); SE (· · ·);

mm and height $h = 3b$. The radius of curvature is $R = 10h$ and the hoop length $S = R\pi$, similarly to previous numerical example. The number of cell is $N_c = 40$. The length of each cell is $L_c = S/N_c$. The unit cell is formed by 35% polymer+30% steel+ 35% polymer, as shown in the Figure 2. A clamped-free boundary condition is applied to the structure. Figure 5 shows the boundary condition and the orientation of excitation force used in the numerical example. Results were obtained using circumferential and radial excitation. Table 1 shows polymer and steel properties.

For the considered case, it was evaluated the dispersion curve of the unit-cell, the forced response and the reaction force. The dispersion curves relates the unit-cell wavenumber versus analyzed frequency band. The wavenumber is calculated as $k_c = i \cdot \ln(\mu)/L_c$ with μ indicating the organized eigenvalue of the transfer matrix. The eigenvalues (wavenumber) and of eigenvectors (mode shape) are organized by the modal assurance criterion (MAC) [19]. The forced response and the reaction force are calculated by Equation 10. It was evaluated the displacement of the three degree of freedom (u, v and ψ) in the Nth cell as showed in the Figure 5. The reaction force is

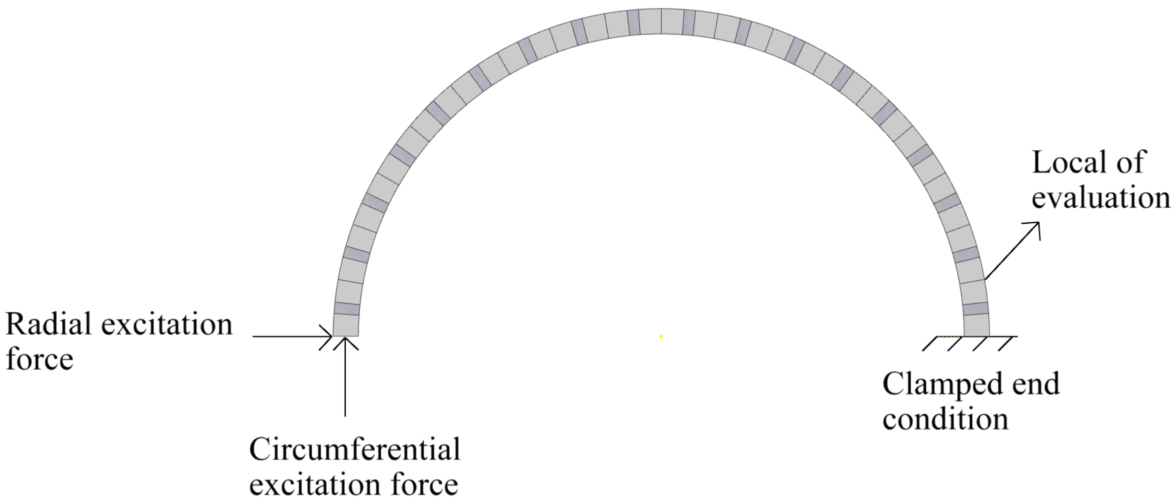

Figure 5: A cantilever PC curved beam with excitation in two different orientation.

Table 1: Phononic Crystal Material Properties.

Property	Steel	Polymer
Elastic Modulus [GPa]	210	3
Density [$\mathrm{kg\,m^{-3}}$]	8030	1340
Poisson's ratio	0.30	0.40
Damping factor	0.001	0.002

evaluated at the clamped end of the structure.

Figure 6 shows the dispersion and receptance curves, respectively. In the graph of dispersion curve, it can see that the curved beam considers propagation of three wave modes. The wavenumber is decomposed into real part ($\Re[k_c L_c]$) and imaginary part ($\Im[k_c L_c]$). The bandgap region is indicated by the shaded areas. At the bandgap region, the real part of wavenumber is equal to π or 0 (Bragg limit) while the imaginary part has a non-zero value indicating a evanescent (non-propagating) wave behavior. As noted, both the circumferential and radial wave modes have two bandgap regions indicated for light blue shaded and gray shaded areas, respectively. As seen in the Figure 6, the receptance curve exposes a considered attenuation at the first circumferential bandgap region (between 23.5-44.3 kHz). In this region the radial mode also presents a bandgap. As can be noted, the circumferential and radial wave modes are related itself. The attenuation only is significant with both circumferential and radial bandgaps are in the same frequency range. Another region where the bandgap modes intersects itself is highlighted in the Figure 6 (between 121-122.4 kHz). Although the imaginary wavenumber part is small, in absolute values, the attenuation is considerable due to the combination of circumferential and radial bandgap.

Figure 7 shows the transmittance curve. As seen, the attenuation behavior is similar to the first case shown in the Figure 6 where the decrease of transmittance values is significantly higher when the two different bandgap occurs simultaneously. However,

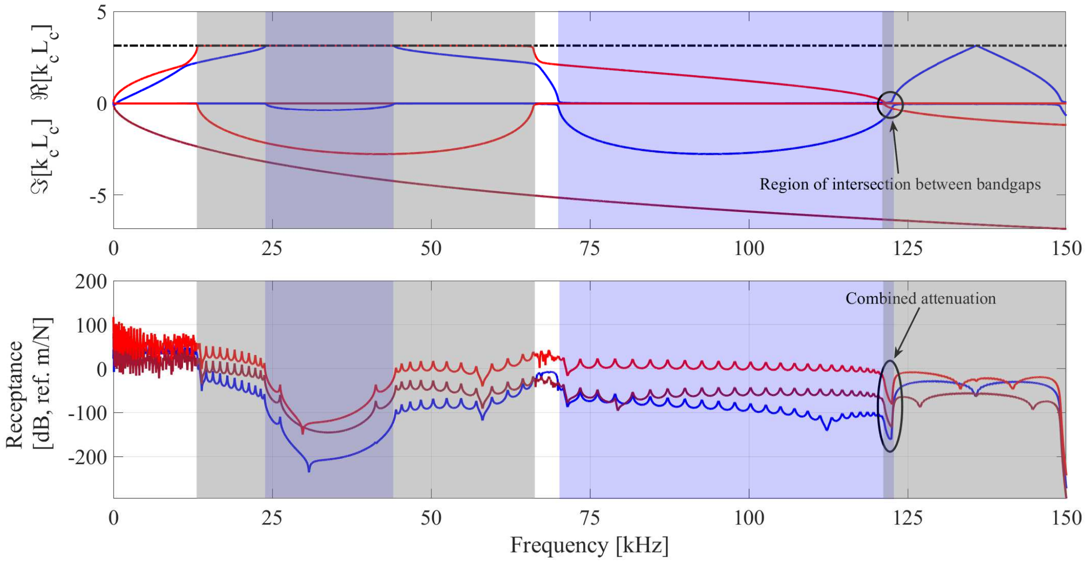

Figure 6: Dispersion curve and forced response for PC curved beam. Circumferential mode (—); Radial mode (—); Rotation mode (—); Bragg limit (- - -).

it can be noted that the transmittance values presents more notable attenuation than in the forced response (Figure 6).

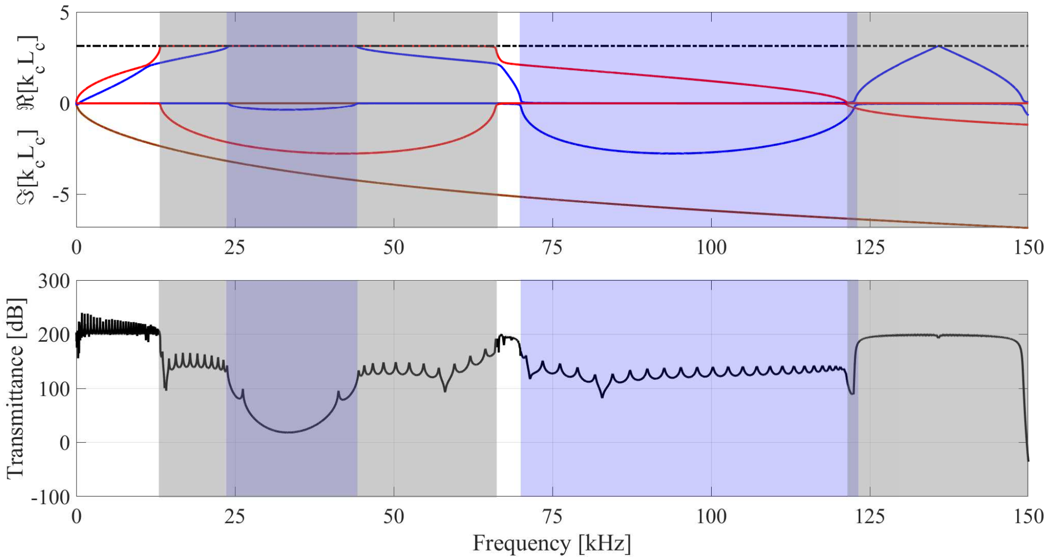

Figure 7: Dispersion curve and transmittance curve for PC curved beam. Circumferential mode (—); Radial mode (—); Rotation mode (—); Reaction circumferential force (—).

5. CONCLUSIONS

The STM approach was proposed as a new procedure to investigate structural phononic crystals using curved Euler-Bernoulli beam theory. The STM methodology involves a transformation of the governing equation in a state-space vector form where the exact wave solutions are not required and allow the direct evaluation of the transfer matrix. Therefore, the ill-conditioned transfer matrix problem is avoided. The wave modes of a periodic structure can be evaluated directly with the transfer matrix eigenvalue problem, then bandgaps can be identified in the dispersion diagram and the attenuation can be evaluated by the forced responses. The STM method was compared with SE method and showed good agreement. The numerical results shows that due to the attenuation between the circumferential and radial modes, the attenuation of the forced response is considerable higher when the bandgap of this two modes occurs simultaneously. The level of attenuation of the forced response do not depends on the orientation of the excitation force due to coupled wave modes present in the curved beam.

6. ACKNOWLEDGEMENTS

The authors are grateful to the Brazilian research funding agencies CAPES, CNPq (Grant No. 313620/2018), FAPEMA (Processo FAPEMA universal-01415/17 and BD-08788/17) and FAPESP for the financial support.

7. REFERENCES

[1] J. C. Delamotte, R. F. Nascimento, and J. R. F. Arruda. Simple models for the dynamic modeling of rotating tires. *Journal of Shock and Vibration*, 1(15):pp. 383–393, 2008.

[2] M. S. Issa, T. M. Wang, and B. T. Hsiao. Extensional vibrations of continuous circular curved beams with rotary inertia and shear deformation, i: Free vibration. *Journal of Sound and Vibration*, 144(2):pp. 297–308, 1987.

[3] C. W. Lim, C. M. Wang, and S. Kitipornchai. Timoshenko curved beam bending solutions in terms of euler-bernoulli solutions. *Archive of Applied Mechanics*, 67(1):pp. 179–190, 1997.

[4] B. Kang, C. H. Riedel, and C. A. Tan. Free vibration analysis of planar curved beams by wave propagation. *Journal of Sound and Vibration*, 1(206):pp. 19–44, 2003.

[5] F. Yang, R. Sedaghati, and E. Esmailzadeh. Free in-plane vibration of curved beam structures: A tutorial and the state of the art. *Journal of Vibration and Control*, 24(12):pp. 2400–2417, 2018.

[6] L. Han, Y. Zhang, Z. Ni, Z. Zhang, and L. Jiang. A modified transfer matrix method for the study of the bending vibration band structure in phononic crystal euler beams. *Physica B*, 407(23):pp. 4579–4583, 2012.

[7] E. J. P. Miranda Jr and J. M. C. Dos Santos. Flexural wave band gaps in phononic crystal euler-bernoulli beams using wave finite element and plane wave expansion methods. *Materials Research*, 3:pp. 1–10, 2018.

[8] D. Garcia-Pablos, M. Sigalas, F. R. Montero de Espinosa, M. Torres, Kafesaki, and N. M., Garcia. Theory and experiments on elastic band gaps. *Physical Review Letters*, 84(19):pp. 4349–4352, 2000.

[9] J. Sanchez-Dehesa and D. Torrent. Acoustic metamaterials based on phononic crystal. *The Journal of the Acoustical Society of America*, 4(128):pp. 2427–2427, 2010.

[10] T. J. R. Hughes. *The finite element method: linear static and dynamic finite element analysis*. Dover, 2000.

[11] J.-M. Mencik and M. Ichchou. Multi-mode propagation and diffusion in structures through finite elements. *European Journal of Mechanics - A/Solids*, 5(24):pp. 877 – 898, 2005.

[12] D. Duhamel, B. Mace, and M. Brennan. Finite element analysis of the vibrations of waveguides and periodic structures. *Journal of Sound and Vibration*, 12(294):pp. 205 – 220, 2006.

[13] E.D. Nobrega, F. Gautier, A. Pelat, and J.M.C. Dos Santos. Vibration band gaps for elastic metamaterial rods using wave finite element method. *Mechanical Systems and Signal Processing*, (76):pp. 192–202, 2016.

[14] J.F. Doyle. *Wave Propagation in Structures: Spectral Analysis Using Fast Discrete Fourier Transforms*. Mechanical Engineering Series. Springer New York, 2012.

[15] U. Lee. *Spectral Element Method in Structural Dynamics*. Wiley, 2009.

[16] D. Rowell. Computing the matrix exponential - the cayley-hamilton method.

[17] D. J. Mead. A general theory of harmonic wave propagation in linear periodic systems with multiple coupling. *Journal of Sound and Vibration*, 2(27):pp. 332–340, 1973.

[18] P. B. Silva, J.-M. Mencik, and Arruda. On the forced response of coupled systems via wfe based super-element approach. In *Proceedings of ISMA*, pages pp.1–13, 2014.

[19] M. Pastor, M. Binda, and T. Harcarik. Modal assurance criterion. *Procedia Engineering*, 1(48):pp. 543–548, 2012.

APPENDIX: EXPRESSION OF THE TRANSFER MATRIX FOR CURVED BEAM

The complete expression for the transfer matrix is given as:

$$
\begin{aligned}
&T_{11} = p_7C_1 + p_8C_2 + p_9C_3 && T_{12} = a\left(\tfrac{p_{11}S_1}{\sqrt{z_1}} + \tfrac{p_{12}S_2}{\sqrt{z_2}} + S_3\sqrt{z_3}(x_{16}+z_3)\right)\\
&T_{13} = a(-p_{29}C_1 + (x_{16}+z_2)C_2 + (x_{16}+z_3)C_3) && T_{14} = \tfrac{p_{18}S_1}{\sqrt{z_1}} + \tfrac{p_{19}S_2}{\sqrt{z_2}} - \tfrac{p_{20}S_3}{z_1z_2z_3^{3/2}}\\
&T_{15} = -a(p_5C_1 + x_{23}C_2 + x_{24}C_3) && T_{16} = ac\left(-\tfrac{p_{29}S_1}{\sqrt{z_1}} + \tfrac{S_2(x_{16}+z_2)}{\sqrt{z_2}} + \tfrac{S_3(x_{16}+z_3)}{\sqrt{z_3}}\right)\\
\\
&T_{21} = ad\left(-\tfrac{p_5S_1}{\sqrt{z_1}} - \tfrac{S_2x_{23}}{\sqrt{z_2}} - \tfrac{x_{24}S_3}{\sqrt{z_3}}\right) && T_{22} = (x_{27}+x_7)C_1 - \mathrm{C2}p_3C_2 + p_4C_3\\
&T_{23} = \tfrac{p_{28}S_3}{q_2\sqrt{z_3}} - \tfrac{p_3S_2}{\sqrt{z_2}} + \tfrac{S_1(x_{27}+x_7)}{\sqrt{z_1}} && T_{24} = a(p_5C_1 + x_{23}C_2 + x_{24}C_3)\\
&T_{25} = \tfrac{p_{24}S_1}{\sqrt{z_1}} - \tfrac{x_{25}S_2}{\sqrt{z_2}} - \tfrac{x_{26}S_3}{\sqrt{z_3}} && T_{26} = c(-x_{33}C_1 + x_{34}C_2 + x_{35}C_3)\\
\\
&T_{31} = -ad(p_5C_1 + x_{23}C_2 + x_{24}C_3) && T_{32} = -\tfrac{p_{13}S_1}{\sqrt{z_1}} + \tfrac{p_{14}\S_2}{\sqrt{z_2}} + \tfrac{p_{15}S_3}{\sqrt{z_3}}\\
&T_{33} = T_{22} && T_{34} = a\left(-\tfrac{p_{21}S_1}{\sqrt{z_1}} + \tfrac{p_{22}S_2}{\sqrt{z_2}} + x_{24}S_3\sqrt{z_3}\right)\\
&T_{35} = p_{24}C_1 - x_{25}C_2 - x_{26}C_3 && T_{36} = cT_{23}\\
\\
&T_{41} = d\left(\tfrac{p_{10}S_3}{z_1z_2\sqrt{z_3}} - \tfrac{p_{30}S_1}{\sqrt{z_1}} + \tfrac{S_2(x_{14}+x_{18})}{\sqrt{z_2}}\right) && T_{42} = ad(C_1(x_2 + 2(z_2+z_3)) - 2(C_2z_2 + C_3z_3))\\
&T_{43} = \tfrac{ad(S_1(x_2+2(z_2+z_3)) - 2\sqrt{z_1}(S_2\sqrt{z_2}+S_3\sqrt{z_3}))}{\sqrt{z_1}} && T_{44} = p_{30}C_1 - (x_{14}+x_{18})C_2 - \tfrac{p_{10}C_3}{z_1z_2}\\
&T_{45} = a\left(\tfrac{p_{25}S_1}{\sqrt{z_1}} - \tfrac{p_{26}S_2}{\sqrt{z_2}} + \tfrac{p_{27}S_3}{z_1z_2\sqrt{z_3}}\right) && T_{46} = -2acd(C_1 + C_2 + C_3)\\
\\
&T_{51} = dT_{13} && T_{52} = d\left(\tfrac{p_{16}S_2}{\sqrt{z_2}} - \tfrac{p_{17}S_3}{\sqrt{z_3}} - \tfrac{S_1(x_{29}+x_5)}{\sqrt{z_1}}\right)\\
&T_{53} = d(x_{21}C_1 - (x_{16}+z_2)C_2 - (x_{16}+z_3))C_3 && T_{54} = a\left(\tfrac{p_{23}S_2 - S_3\sqrt{z_2}\sqrt{z_3}(x_{16}+z_3)}{\sqrt{z_2}} - \tfrac{p_{11}S_1}{\sqrt{z_1}}\right)\\
&T_{55} = T_{22} && T_{56} = cd\left(\tfrac{x_{x21}S_1}{\sqrt{z_1}} - \tfrac{(x_{16}+z_2)S_2}{\sqrt{z_2}} - \tfrac{(x_{16}+z_3)S_3}{\sqrt{z_3}}\right)\\
\\
&T_{61} = ad\left(\tfrac{p_{29}S_1}{\sqrt{z_1}} - \tfrac{(x_{16}+z_2)S_2}{\sqrt{z_2}} - \tfrac{(x_{16}+z_3)S_3}{\sqrt{z_3}}\right) && T_{62} = d(-x_{21}C_1 + (x_{16}+z_2)C_2 + (x_{16}+z_3)C_3)\\
&T_{63} = d\left(-\tfrac{x_{21}S_1}{\sqrt{z_1}} + \tfrac{(x_{16}+z_2)S_2}{\sqrt{z_2}} + \tfrac{(x_{16}+z_3)S_3}{\sqrt{z_3}}\right) && T_{64} = T_{13}\\
&T_{65} = -\tfrac{p_{28}S_3}{q_2\sqrt{z_3}} + \tfrac{p_3S_2}{\sqrt{z_2}} - \tfrac{(x_{x27}+x_7)S_1}{\sqrt{z_1}} && T_{66} = x_{36}C_1 + x_{37}C_2 + x_{38}C_3
\end{aligned}
\tag{A.1}
$$

The terms z_1, z_2 and z_3 are roots of the polynomial given below:

$$
\xi^3 + (2a^2 + bd)\xi^2 + (a^4 - a^2bd - cd) * \xi + (a^2cd - bcd^2), \tag{A.2}
$$

where

$$
\begin{aligned}
a &= \frac{1}{R} \quad b = \frac{1}{EA}\\
c &= \frac{1}{EI} \quad d = \rho\, A\, \omega
\end{aligned}
\tag{A.3}
$$

And the auxiliary terms used in the expressions are described in the A.4, A.5 and A.6:

$$
\begin{aligned}
x_1 &= a^4 - (a^2b + c)d & x_2 &= 4a^2 + 2bd \\
x_3 &= 2a^2b + c + b^2d & x_4 &= a^4 + 4a^2bd + b^2d^2 \\
x_5 &= 5a^4 + 4a^2bd + cd & x_6 &= a^4 + 6a^2bd \\
x_7 &= a^4 + 2a^2bd + cd & x_8 &= 4a^8 - 2a^6bd + a^2bcd^2 - a^4d(7c + 2b^2d) \\
x_9 &= a^4 + 5a^2bd + 3cd & x_{10} &= -a^6 + a^4bd + a^2cd \\
x_{11} &= -5a^4 - a^2bd + cd & x_{12} &= 2a^2b + 2c + b^2d \\
x_{13} &= z_1z_2 + (a^2 - bd)(a^2 + z_3) & x_{14} &= a^4 - a^2bd \\
x_{15} &= a^2 + 2bd + z_2 + z_3 & x_{16} &= a^2 - bd \\
x_{17} &= a^2 + 2bd & x_{18} &= (a^2 + bd)z_2 - z_1z_3 \\
x_{19} &= (a^2 + bd)z_3 & x_{20} &= z_2(a^2 + bd + z_3) \\
x_{21} &= 3a^2 + z_2 + z_3 & x_{22} &= d(c + 2b^2d) \\
x_{23} &= c - bz_2 & x_{24} &= c - bz_3 \\
x_{25} &= bcd + (a^2b + c)z_2 & x_{26} &= bcd + (a^2b + c)z_3 \\
x_{27} &= a^2z_3 + z_2(a^2 + z_3) & x_{28} &= a^6 - a^4bd - 2a^2cd + bcd^2 \\
x_{29} &= 3a^2z_3 + z_2(3a^2 + z_3) & x_{30} &= 3a^4b + b^3d^2 + a^2(c + 5b^2d) \\
x_{31} &= a^2(-a^2b + c + b^2d) & x_{32} &= 3a^4b + bd(2c + b^2d) + a^2(2c + 5b^2d) \\
x_{33} &= a^2 + z_2 + z_3 & x_{34} &= a^2 + bd + z_2 \\
x_{35} &= a^2 + bd + z_3 & x_{36} &= cd + z_2z_3 \\
x_{37} &= cd + z_1z_3 & x_{38} &= cd + z_1z_2 \\
x_{39} &= a^2(13a^2b + 7c)d + 2b(2a^2b + c)d^2
\end{aligned}
\tag{A.4}
$$

$$
\begin{aligned}
p_1 &= x_8 + (x_9 + (7a^2 + 2bd)z_1)z_2^2 & p_2 &= z_2(a^6 + x_{39} + x_{11}z_3) \\
p_3 &= x_1 + a^2z_2 - z_1z_3 & p_4 &= x_7 + a^2z_1 + (a^2 + z_1)z_2 \\
p_5 &= x_3 + b(z_2 + z_3) & p_6 &= x_{10} + x_{11}z_1 \\
p_7 &= z_2(bd + z_3) + bd(\tfrac{x_2}{2} + z_3) & p_8 &= -bdz_2 + z_1z_3 \\
p_9 &= bd(\tfrac{x_2}{2} + z_1) + (bd + z_1)z_2 & p_{10} &= cd(z_1z_2 + x_{16}(a^2 + z_3)) \\
p_{11} &= x_{22} + x_6 + x_{17}z_3 + z_2(x_{17} + z_3) & p_{12} &= -x_1 - x_{17}z_2 + z_1z_3 \\
p_{13} &= a^2(4cd + 2b^2d^2 + x_6) + x_7z_3 + z_2(x_7 + a^2z_3) & p_{14} &= x_{28} + x_7z_2 - a^2z_1z_3 \\
p_{15} &= cdx_{16} + z_3(-x_1 - a^2z_3) & p_{16} &= x_1 + 3a^2z_2 - z_1z_3 \\
p_{17} &= x_5 + 3a^2z_1 + (3a^2 + z_1)z_2 & p_{18} &= x_{30} + \tfrac{1}{2}bx_2z_3 + bz_2(\tfrac{x_2}{x} + z_3) \\
p_{19} &= x_{31} - \tfrac{1}{2}bx_2z_2 + bz_1z_3 & p_{20} &= cdx_{16}(a^2c - bcd + bz_3^2) \\
p_{21} &= x_{32} + x_3z_3 + z_2(x_3 + bz_3) & p_{22} &= bx_1 + x_3z_2 - bz_1z_3 \\
p_{23} &= x_1 + x_{17}z_2 - z_1z_3 & p_{24} &= a^2x_{12} + (a^2b + c)(z_2 + z_3) \\
p_{25} &= 2cd + x_{19} + x_{20} + x_4 & p_{26} &= -2cd + x_{14} + x_{18} \\
p_{27} &= cd(z_1z_2 - x_{16}(a^2 + z_3)) & p_{28} &= p_1 + p_2 + 3z_1z_2^3 + p_6z_3 \\
p_{29} &= x_{17} + z_2 + z_3 & p_{30} &= x_{19} + x_{20} + x_4
\end{aligned}
\tag{A.5}
$$

$$
q_1 = x_1 + z_1(x_2 + 3z_1) \quad q_2 = x_1 + z_2(x_2 + 3z_2) \quad q_3 = x_1 + z_3(x_2 + 3z_3) \tag{A.6}
$$